Comparative Study of Dust Properties around White Dwarf PG 1225-079 in IRIS, AKARI and WISE Data

S. Sigdel, S. Rijal and M. S. Paudel

Journal of Nepal Physical Society

Volume 8, Issue 3, December 2022

ISSN: 2392-473X (Print), 2738-9537 (Online)

JNPS, **8** (3): 79-92 (2022)

DOI: https://doi.org/10.3126/jnphyssoc.v8i3.50750

Published by:

Nepal Physical Society
P.O. Box: 2934
Tri-Chandra Campus
Kathmandu, Nepal
Email: nps.editor@gmail.com

JNPS 8 (3): 79-92 (2022)
ISSN: 2392-473X (Print), 2738-9537 (Online)

Research Article *© Nepal Physical Society*
DOI: https://doi.org/10.3126/jnphyssoc.v8i3.50750

Comparative Study of Dust Properties around White Dwarf PG 1225-079 in IRIS, AKARI and WISE Data

S. Sigdel, S. Rijal and M. S. Paudel*
Department of Physics, Tri-Chandra Multiple Campus, Tribhuvan University, Kathmandu, Nepal
*Corresponding Email: mspaudel27@gmail.com, madhu.paudel@trc.tu.edu.np

Received: *3rd July, 2022;* ***Revised:*** *12th Oct., 2022;* ***Accepted:*** *3rd Dec., 2022*

ABSTRACT

In this work, dust properties around the White Dwarf PG 1225-079 located at RA (J2000): 12^h 27^m 47.35^s, DEC(J2000): -08° 14' 37.97" is studied extensively using the publicly available data from Improved Reprocessing of IRAS Survey (IRIS), AKARI infrared survey and Wide field Infrared Survey Explorer (WISE). The bipolar dust structure hardly resolved in IRIS (60 μm and 100 μm) is clearly resolved in AKARI (90 μm and 140 μm) and WISE (12 μm and 22 μm) images. The dust color temperature and dust mass are calculated from the infrared flux density. The average value of dust color temperature in isolated dust structure is 27.57 K for IRIS (I1). For isolated upper and lower dust clouds the average temperatures are; 22.64 K and 22.63 K for AKARI (A1 and A2), 295.34 K and 296.85 K in WISE (W1 and W2) data. A wide range of temperatures suggests the bipolar dust structure is dynamically active. The mass of dust is found to be 3.44×10^{25} kg in IRIS (I1), 1.82×10^{26} kg and 5.89×10^{26} kg in two bipolar regions in AKARI (A1 and A2) and 1.12×10^{26} kg and 1.14×10^{26} kg in WISE (W1 and W2). A good relation is found between the infrared flux in all survey data with r^2 value 0.83 in IRIS (I1) and more than 0.90 in AKARI (A1, A2) and WISE (W1, W2) data. SIMBAD database explore some sources including Supernova Remnants nearby the dust which might be the progenitor of dust as well as the contributor of energetic radiation. The Gaussian modeling of temperature is found to be deviated from normal shape. The contour plot of dust color temperature and dust mass shows non uniform variation among the IRIS, AKARI and WISE survey. The relation between infrared flux, dust color temperature and dust mass within the dust clouds are presented.

Keywords: PG 1225-079, Dust Cloud, Dust Color Temperature, Dust Mass, IRIS, AKARI, WISE.

INTRODUCTION

Interstellar dusts are the tiny but important component of the interstellar medium (ISM). The Asymptotic Giant Branch (AGB) phase of stellar evolution is inferred for the majority of the known dust formation process for the low to intermediate mass star ($0.8\ M_\odot < M < 8\ M_\odot$) [1]. The other violent process, for intense; supernova explosion [2] is the analogous phase used to infer for the source of dust for massive stars ($M > 25\ M_\odot$). The processes of growth, coagulation, erosion, shattering, etc., are the processes which increase the abundance of dust within the ISM [3]. The major fraction of the dust consists of silicate, carbon and hydrocarbon molecules, with a size ranging from 0.01 μm to 0.1 μm. The formation process of some abundant dust component are still unknown, for example; polyaromatic hydrocarbon (PAH). Dust is important in many processes, including gas thermodynamics and chemistry, dynamics of star formation, and determines the spectra of galaxy, re-radiating the absorbed short wavelength electromagnetic (EM) radiating into long wavelength infrared radiation. The dust grains are able to absorb EM radiation with a wavelength smaller than the diameter of the dust grains. The extinction caused by dust depends mainly on the column density. The regions in ISM where the light from background star is completely blocked are

called the *dark nebula* where as those regions which scatters the background radiation from star are called the *reflection nebula*. [4]

The mid and far-infrared emission from the dust particles provides a bunch of hidden secrets within the nebula. The Infrared Astronomical Satellite (IRAS), launched in 1983, is the first space satellite designed exclusively for this purpose [5]. The Japanese AKARI infrared survey [6] and NASA's Wide Field Infrared Explorer (WISE) [7] also work in the mid and far-infrared fields with greater resolution. There has been a lot of research done using IRAS data to investigate the dust color temperature and dust mass using far-infrared data at 60 μm and 100 μm wavelength. Thapa *et al.* 2019 [8] studied two isolated dust emission nebulae at Galactic coordinate (353.01^0, 16.98^0), and (18.42^0, 1.98^0). The average temperature is obtained at 27.92 K and 31.61 K with a wide range of temperature of 15.15 K and 23.11 K respectively. The study of the infrared cavity nearby the White Dwarf WD 352-249 shows the mean dust color temperature at 23.09 K with a range of 2.22 K using the IRAS data. The small variation in temperature infers that the dust cavity is evolving independently and less disturbed from the background radiation source [9]. The study of dust sub- structures around White Dwarf WD 0307+077 found that the dust temperature between 20 K to 24 K with range no more than 3 K[10]. A study of dust cavity near the Pulsar at Galactic latitude: -60^0 shows the variation of dust color temperature from 22.78 K to 24.78 K, implying that the cavity structure is less disturbed from nearby Pulsar and it's radiation [11]. The study of FIR loop (cavity) at Galactic latitude: -5^0 near the Pulsar J1627- 5547 shows a temperature variation of 16 K suggesting the cavity is dynamically active, which consists of a more stable core region having a temperature variation of less than 3 K [12]. In a study using Improved Reprocessing of IRAS Survey (IRIS) and AKARI infrared survey data, the infra-red study of isolated dust structure, located at Galactic latitude 0.04^0 nearby supernova remnants G053.41+00.3, G053.9+00.2 and G053.1+00.3, found a large fluctuation of dust color temperature of more than10 K[13]. The average dust color temperature for IRIS and AKARI data is 25.66 K and 17.74 K, decreasing for longer wavelengths, following the Wein's displacement law. Numerous background sources are explored in the SIMBAD database and it is declared that these sources are responsible for the large variation in temperature violating the local thermodynamic equilibrium.

In this work, a systematic search in Sky View Virtual Observatory (www.skyview.gsfc.nasa.gov) revealed interesting isolated nebular structure nearby the White Dwarf in IRIS, AKARI and WISE database. Such an interesting bipolar emission dust nebula is observed in mid and far-infrared wavelengths of all IRIS, AKARI, and WISE data nearby the White Dwarf PG 1225-079, which is a very rare scenario. The dust nebula, which is very hardly resolved in IRIS data at 60 µm and 100 µm but easily resolved into the bipolar structure in AKARI 90 µm and 140 µm and WISE 12 µm and 22 µm data as shown in Fig.1.

The main objective of this work is to calculate the dust color temperature, dust mass, inclination angle, and Jeans mass within the bipolar nebula and study the relationship between infrared flux, dust color temperature, and dust mass within it. On the basis of the result the possible ongoing physical processes within the dust cloud is discussed.

SOURCES OF DATA

The IRIS data [14] at 60 μm and 100 μm, AKARI data [6] at 90 μm and 140 μm and WISE data [7] at 12 μm and 22 μm are taken from Sky View Virtual Observatory (https://skyview.gsfc.nasa.gov). The SIMBAD (http://simbad.u-strasbg.fr/simbad/ sim-fcoo) is used for the study of background objects embedded within the dust structure and the determination of the distance to the White Dwarf PG 1225-079.

METHOD OF ANALYSIS

Dust Color Temperature and Dust Mass

The interstellar dust absorbs the radiation from the nearby sources and re-radiates the absorbed energy as thermal radiation in the infrared band of electromagnetic radiation. The concept of blackbody emission can be used to estimate the dust color temperature following Wood *et al.* (1994) [15] and Schnee *et al.* (2005) [16]. The final expression of the dust color temperature is given as;

$$T_d = -\frac{p}{\ln\{R \times q^{3+\beta}\}} \quad \text{.....(1)}$$

Where, R = F(short)/F(long), and F(short) = F(60 μm) for IRIS, F(90 μm) for AKARI and F(12 μm) for WISE and F(long) = F(100 μm) for IRIS, F(140 μm) for AKARI and F(22 μm) for WISE, p = 96 for IRIS, 57 for AKARI,

545.13 for WISE, and q = 0.6 for IRIS, 0.64 for AKARI and 0.55 for WISE, β is the spectral emissivity index which takes the values from 0 to 2 [17]. The longer wavelength can give the precious measurement of mass of the dust particles [16]. Therefore, the long wavelength infrared flux is used for the measurement of dust mass following Young *et al*. (1993) [18] and Hildebrand (1983) [19]. The expression for the calculation of the mass of dust is;

$$M_{dust} = 0.4\left[\frac{S_\nu D^2}{B(\nu,T_d)}\right] \quad \text{.....(2)}$$

Where, S_ν is the flux density in SI unit = f × MJy/Str × 5.288 × 10^{-9}, 1 MJy/Str = 1 ×10^{-20} kg s^{-2}, f is the flux density, D is the distance to the dust structure and B (ν, T_d) is the Planck's function. To calculate the total mass of cloud including gas, we consider that the mass of cloud with gas is 200 times of the mass of the dust [19].

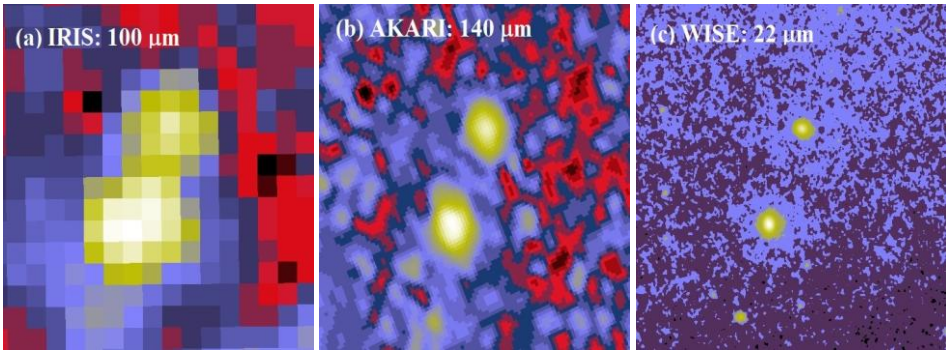

Fig.1: The figure shows the JPEG image of the dust structure in IRIS at 100 μm (a), AKARI at 140 μm (b) and WISE at 22 μm (c) data, all 0.4^0 ×0.4^0 in size, centered at RA(ICRS): 186.87^0, DEC.(ICRS): -08.23^0. In IRIS data the dust structure is single and elongated but in AKARI and WISE it is clearly resolved into bipolar structures. Source: Sky View Virtual Observatory

Size, Density and Jeans Mass

The angular size of major and minor axis, θ, is converted into linear size, L, by using $L = D \times \theta$, where, D is the distance to the dust structure. The average value of major and minor axis is used to calculate the density, ρ, of the dust, given as;

$$\rho = \left(\frac{3}{4\pi}\right)^{2/3} \frac{k_B T_d}{m_H G R^2} \quad \text{..... (3)}$$

Where, Boltzmann constant (k_B) =1.38 ×10^{-23}J K^{-1}, T_d is the average temperature, R is the average radius of dust cloud, mean molecular mass of hydrogen gas (m_H) =1.67 10^{-27} kg and Gravitational constant (G) = 6.67 10^{-11} N m^2 kg^{-2}.

The Jeans mass of the cloud is calculated using;

$$M_J = \left(\frac{k_B T_d}{m_H G}\right)^{3/2} \frac{1}{\rho^{1/2}} \quad \text{..... (4)}$$

If the mass of the dust cloud is greater than Jeans mass, the dust cloud will leads towards the star formation process in the future, otherwise the star formation process will vanish [4].

Inclination Angle

The inclination angle (i) is the representation of the visual angle, which can be defined as the angle made by the direction of visualization to the normal of the plane of the dust cloud. The Holmberg (1946) [20] formula enables us for the calculation of inclination angle, which is given as;

$$\cos^2 i = \frac{\left(\frac{b}{a}\right)^2 - q^{*2}}{1 - q^{*2}} \quad \text{.....(5)}$$

Where, $\frac{b}{a}$ is the ratio of minor to major axis and q* is the intrinsic flatness of the structure. In this work, the value of intrinsic flatness q* is taken to be 0.23 [21] for molecular cloud. The inclination angle decides whether the dust structure is *edge−on*; having a value more than 45^0 or *face−on*; having a value less than 45^0.

RESULTS AND DISCUSSION

Dust Structure and Sub-structures

In IRIS data, the isolated dust structure nearby the dust White Dwarf PG 1227-079 appears single and elongated along North-to-South. But in AKARI and WISE data, it is well resolved into bipolar sub-structures. The upper and lower bipolar sub-structures are named as; A1 and A2 in AKARI, W1 and W2 for WISE respectively and the single elongated dust structure in IRIS data is named as I1 all over this work. The sub−structures A1, A2, W1

and W2 are studied separately. Table 1 gives the coordinate of the center, size, number of pixels, and size of the isolated region of I1, A1, A2, W1 and W2 under study. It is seen that the size of isolated structures in WISE are smaller in comparison to AKARI data.

Infrared Flux Density, Dust Color Temperature and Mass

The infrared flux is the basic parameter in this work. We have calculated the dust color temperature and dust mass from infrared flux. The flux density is extracted from the software Aladin v11.0 [22]. The Table 2 contains detail statistical information of infrared flux within all structures at both wavelengths. It can be seen that the flux density in WISE (W1 and W2) is greater than AKARI (A1 and A2) and smallest in IRIS (I1). The maximum, minimum, mean, range, and standard error (SE) of dust color temperature within the dust cloud I1, A1, A2, W1 and W2 are presented in Table 3.

Table 1: The table gives center, size of total region, number of pixels in total region and size of isolated region. The total region is square in shape.

Name	Center (RA, DEC.) (ICRS)	Total Size	Pixels	Isolated Size
I1	186.87^0, -08.23^0	0.50^0	400	$22.51' \times 10.59'$
A1	186.91^0, -08.28^0	0.10^0	576	$3.74' \times 2.74'$
A2	186.87^0, -08.17^0	0.07^0	289	$5.50' \times 3.51'$
W1	189.91^0, -08.27^0	0.03^0	6400	$1.51' \times 1.28'$
W2	186.86^0, -08.16^0	0.03^0	6400	$1.31' \times 1.29'$

Table 2: The table gives the maximum, minimum, mean and range of infrared flux at different wavelength within I1, A1, A2, W1 and W2.

Name	λ (μm)	F*max* (MJy/sr)	F*min* (MJy/sr)	F*mean* (MJy/sr)	Range (MJy/sr)
I1	60	10.25	0.52	1.05	9.73
	100	15.10	2.27	3.08	12.84
A1	90	32.36	4.32	9.41	28.04
	140	47.59	2.48	10.84	45.11
A2	90	80.73	2.22	9.43	78.51
	140	111.02	2.00	11.55	109.01
W1	12	1244.68	747.48	771.79	497.20
	22	266.44	250.31	251.84	16.13
W2	12	1696.31	747.82	791.35	948.49
	22	303.80	252.32	256.31	51.48

Total represents the entire square region of a given size and *Isolated* represents an isolated core region observed in infrared flux at long wavelength (100 μm in I1, 140 μm in A1 and A2 and 22 μm in W1 and W2). The isolated region of flux at the respective wavelength can be seen in the contour plot in Fig. 2. The average temperature of isolated region is less than the total region in I1, W1 and W2, but for A1 and A2 it is more than the total region. It means, in A1 and A2, the hot dust lies outside the isolated region, but in I1, W1 and W2, the hot dust lies inside the isolated region. In the isolated region, the average temperature is found to be increased for every decrease in wavelength. The average temperature is highest for WISE data (12 and 22 μm) and lowest for AKARI data (90 and 140 μm). This result follows Wien's displacement law. The range of the dust color temperature in isolated region is more than 5 K in all structures. This indicates that the dust within the structure is not in local thermodynamic equilibrium, the region is thermally dynamic. The objects embedded within the dust structure might be playing major roles in the thermal activity.

Table 3: The table shows the maximum, minimum, mean, range and standard error (σ/√n) of the dust color temperature within I1, A1, A2, W1 and W2.

Name	Region	T_{max} (K)	T_{min} (K)	T_{mean} (K)	Range (K)	SE (K)
I1	Total	34.58	22.91	25.84	11.67	0.07
	Isolated	34.58	24.02	27.57	10.56	0.33
A1	Total	43.47	20.33	26.82	23.14	0.30
	Isolated	26.53	20.33	22.64	6.20	0.10
A2	Total	42.74	17.87	27.68	24.87	0.22
	Isolated	27.40	17.87	22.63	9.53	0.15
W1	Total	376.55	287.51	291.56	89.04	0.14
	Isolated	376.55	287.74	295.34	88.81	0.26
W2	Total	429.46	286.38	292.46	143.08	0.21
	Isolated	429.46	286.59	296.85	142.86	0.35

For the calculation of the mass we need the distance. The distance to PG 1225-079 taken from the Vizier on- line data catalogue is 32.73 pc [23]. This distance is used for the calculation of the dust mass in each pixel. The sum of the mass of dust of all the pixels gives the total mass of the dust within the structure. The mass of the dust cloud including gas is about 200 times greater than the mass of the dust [19]. Using this concept, the total mass of cloud within the structure is calculated. The dust mass and total cloud mass within the total and isolated region are presented in Table 4. The dust mass in AKARI (A1, A2) and WISE (W1, W2) data is in same order, where as in IRIS (I1) it is one order less than AKARI (A1, A2) and WISE (W1, W2) data. In the total region it is found that the mean mass per pixels is found 8.59×10^{22} kg for I1, 1.02×10^{24} kg for A1, 6.57×10^{23} kg for A2, 1.77×10^{22} kg for W1 and 1.75×10^{22} kg for W2.

Table 4: The table gives the mass of dust and gas within the total and isolated region of I1, A1, A2, W1 and W2.

Name	Quantity	Total region (kg)	Isolated region (kg)
I1	M_{dust}	3.44×10^{25}	6.53×10^{24}
	M_{gas}	6.87×10^{27}	1.31×10^{27}
A1	M_{dust}	1.82×10^{26}	1.66×10^{26}
	M_{gas}	3.63×10^{28}	3.32×10^{28}
A2	M_{dust}	5.89×10^{26}	5.60×10^{26}
	M_{gas}	1.18×10^{29}	1.12×10^{29}
W1	M_{dust}	1.12×10^{26}	5.48×10^{25}
	M_{gas}	2.24×10^{28}	1.10×10^{28}
W2	M_{dust}	1.14×10^{26}	6.32×10^{25}
	M_{gas}	2.27×10^{28}	1.26×10^{28}

Contour Map of Infrared Flux, Temperature and Mass

The contour plot of infrared flux, dust color temperature, and dust mass for all dust clouds I1, A1, A2, W1 and W2 are presented in Fig. 2, Fig. 3 and Fig. 4 respectively. In all clouds, the maximum flux is seen near the center and gradually decreases at outwards. In I1, the unresolved bipolar structure can be seen single and elongated along North−to−South in contour plot of infrared flux, which is separated into A1 and A2 in AKARI data and W1 and W2 in WISE data. In W1 and W2, the infrared flux is smooth varying from center to outside, which is due to the higher resolution of WISE image than AKARI and IRIS image.

The contour map of dust color temperature is different than the infrared flux and enclosing the intricate infrared features. In I1, W1 and W2, the temperature is high towards the center, but in A1 and A2 it is less towards the center. The contour map of dust mass is neither similar to flux nor similar to dust color temperature. In I1, A1 and A2, the heavy dust is closer to the center whereas lighter dust lies towards the center in W1 and W2. In W1 and W2, a pair of bean shaped massive regions is observed on both sides from center, in the direction transverse to the direction of elongation of dust cloud, which is unique among all structures.

Relation between Infrared Flux, Temperature and Mass

The contour map with color shows the relationship between the infrared flux, dust color temperature and dust mass in a qualitative way. Their relationship can be studied quantitatively using polynomial regression. We have presented the results of only those plots in which the regression coefficient (r^2) is

greater than 0.5. In I1, A1 and A2, the best fit relationship between the infrared flux is seen as linear but in W1 and W2; it is found to be parabolic, as shown in Fig. 5. In all, it can be said that the infrared flux produced from dust grains at both wavelengths increases simultaneously. The relationship between the dust color temperature and infrared flux is presented in Fig. 6. In I1, W1 and W2 there is the positive correlation and in A1 and A2 there is negative correlation between temperature and flux. The relationship between the dust mass and infrared flux is presented in Fig. 7. In I1, there is bad fit between infrared flux and mass, not shown in figure. In A1 and A2, the mass is directly proportionality to flux; r^2 is more for the long wavelengths (140 μm). For W1 and W2, the mass depends inversely on the flux in both wavelengths (12 μm and 22 μm), r^2 is found more for short wavelength (12 μm) flux. The relationship between the infrared flux and mass is contradictory in AKARI and WISE data. This might be due to the fact that the AKARI data are at far-infrared wavelength whereas the WISE data are at mid-infrared wavelength. Also, the WISE data are more focused within the small region in comparison to AKARI data, for intense; the size of A1, A2, W1 and W2 can be seen in Table 1.

The relation between dust colors temperature and dust mass is presented in Fig. 8. In I1, there is bad fit between them, not shown in figure. In A1 and A2, the mass depends inversely with temperature; r^2 is more for A1 in general. But an intense view of the data shows that there is combination of the two features in both graphs Fig. 8(a) and Fig.8(b). The first set of data is that which have high value of dust mass but lower dust color temperature, approximately less than 25 K. The second set represents the data having lower dust mass and higher dust color temperature, approximately more than 25 K.

Table 5: The variables for the linear and polynomial fit and their regression coefficient (r^2) is presented. X and Y represents the variable along X and Y axis respectively.

	X	Y	Nature	r^2
I1	F(100μm)	F(60μm)	Linear	0.92
A1	F(140μm)	F(90μm)	Linear	0.95
A2	F(140μm)	F(90μm)	Linear	0.93
W1	F(22μm)	F(12μm)	Parabolic	0.99
W2	F(22μm)	F(12μm)	Parabolic	0.98
I1	F(60μm)	T_d	Parabolic	0.69
A1	F(140μm)	T_d	Polynomial	0.66
A2	F(140μm)	T_d	Polynomial	0.82
W1	F(12μm)	T_d	Linear	1.0
	F(22μm)	T_d	Parabolic	0.99
W2	F(12μm)	T_d	Linear	1.0
	F(22μm)	T_d	Parabolic	0.96
A1	F(90μm)	Mass	Linear	0.84
	F(140μm)	Mass	Linear	0.93
A2	F(90μm)	Mass	Linear	0.53
	F(140μm)	Mass	Linear	0.76
W1	F(12μm)	Mass	Linear	0.99
	F(22μm)	Mass	Parabolic	0.97
W2	F(12μm)	Mass	Linear	0.92
	F(22μm)	Mass	Parabolic	0.84
A1	T_d	Mass	Polynomial	0.83
A2	T_d	Mass	Polynomial	0.73
W1	T_d	Mass	Linear	0.99
W2	T_d	Mass	Linear	0.95

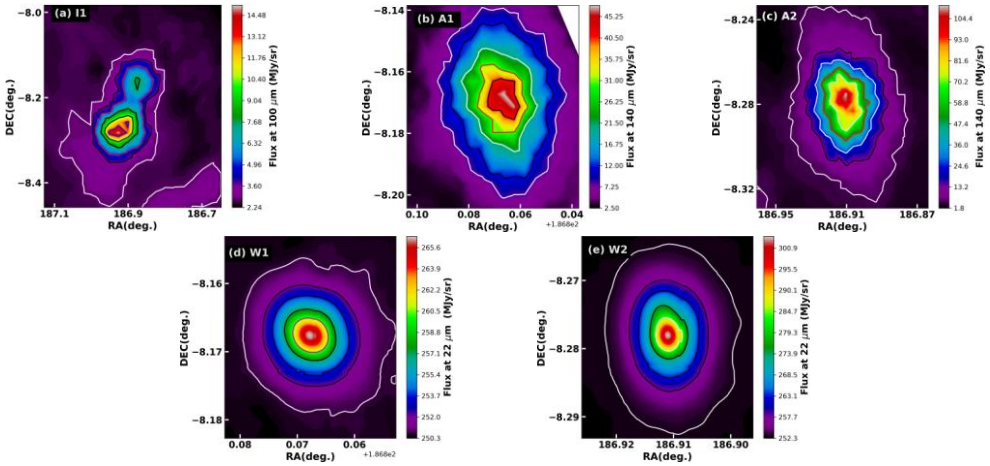

Fig. 2: The figure shows the contour map for infrared flux in (a) I1 at 100 μm, (b) A1 and (c) A2 at 140 μm (d) w1 and (e) W2 at 22 μm. The lines represent the isocontours.

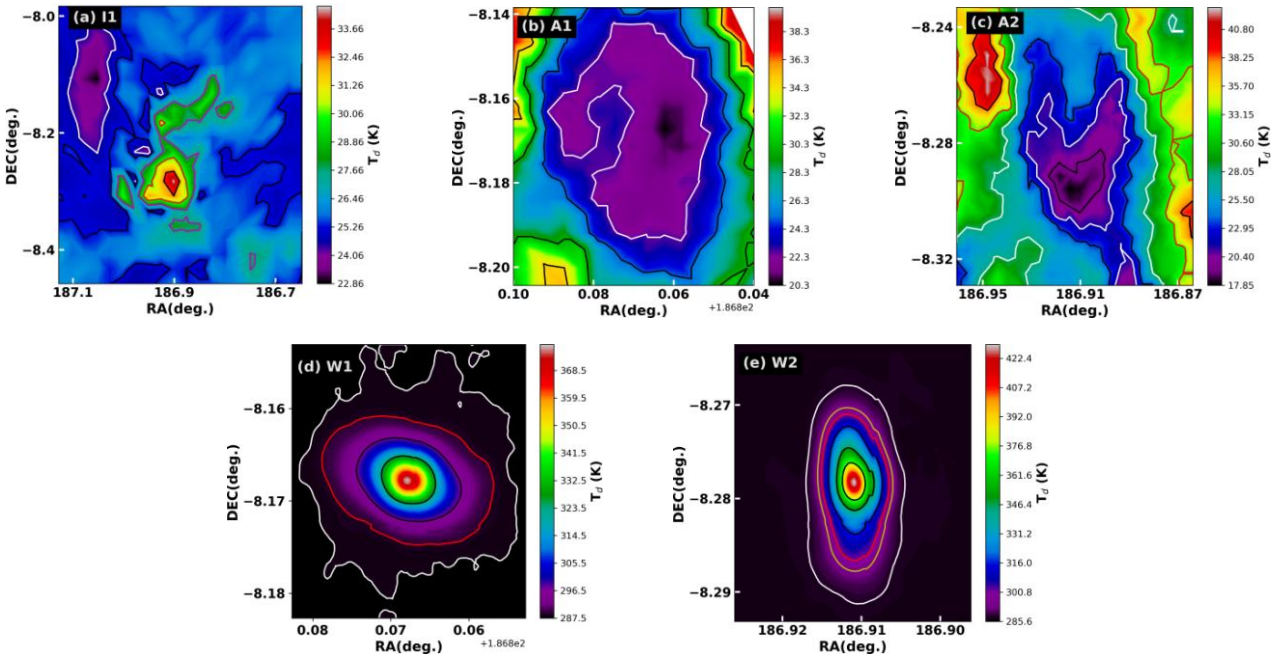

Fig. 3: The figure shows the contour map of dust color temperature for I1, A1, A2, W1 and W2. The lines represent the isocontours.

By comparing the contour plot of mass and temperature it can be said that the first set of data belongs to the dust in the central region and second set of data belongs to the dust in the outer regions. That means the dust in the central region and outer regions have different infrared features in AKARI data. For W1 and W2, the mass depends inversely on the temperature for entire regions, r^2 is found more for W1.

SIMBAD Sources

The SIMBAD database provides the identified objects within the selected region. The OTYPE and their numbers are presented in the Table 6 and can be visualized in Fig. 9. There are a large number of sources within I1, but in A1, A2, W1 and W2, the number of SIMBAD sources are very less because of their small angular size.

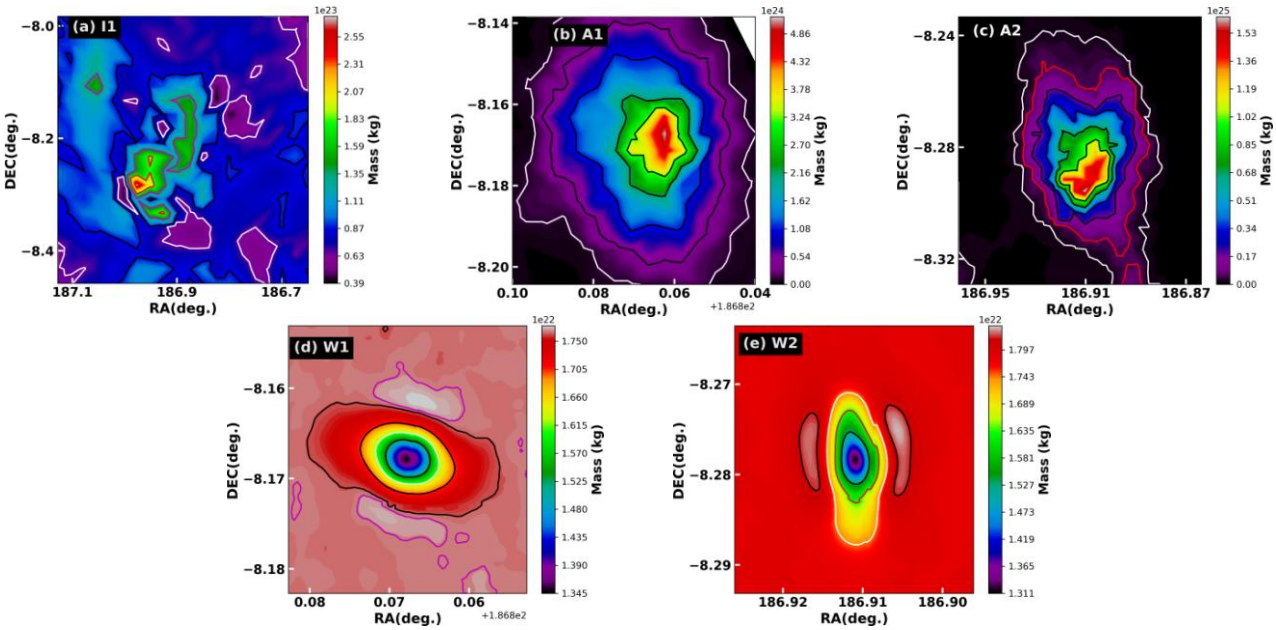

Fig.4: The figure shows the contour plot for dust mass in I1, A1, A2, W1 and W2. The lines represent the isocontours.

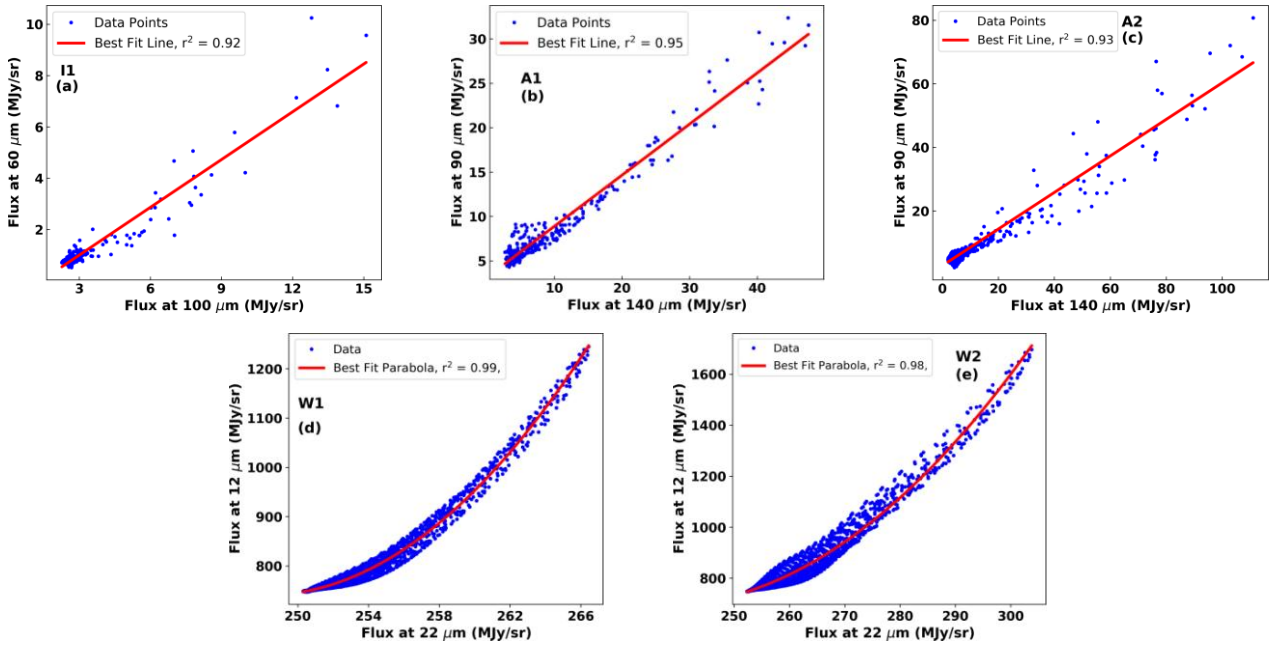

Fig. 5: Figure shows the relation between infrared flux at two wavelength (60 μm and 100 μm in I1, 90 μm and 140 μm in A1 and A2, and 12 μm and 22 μm in W1 and W2).

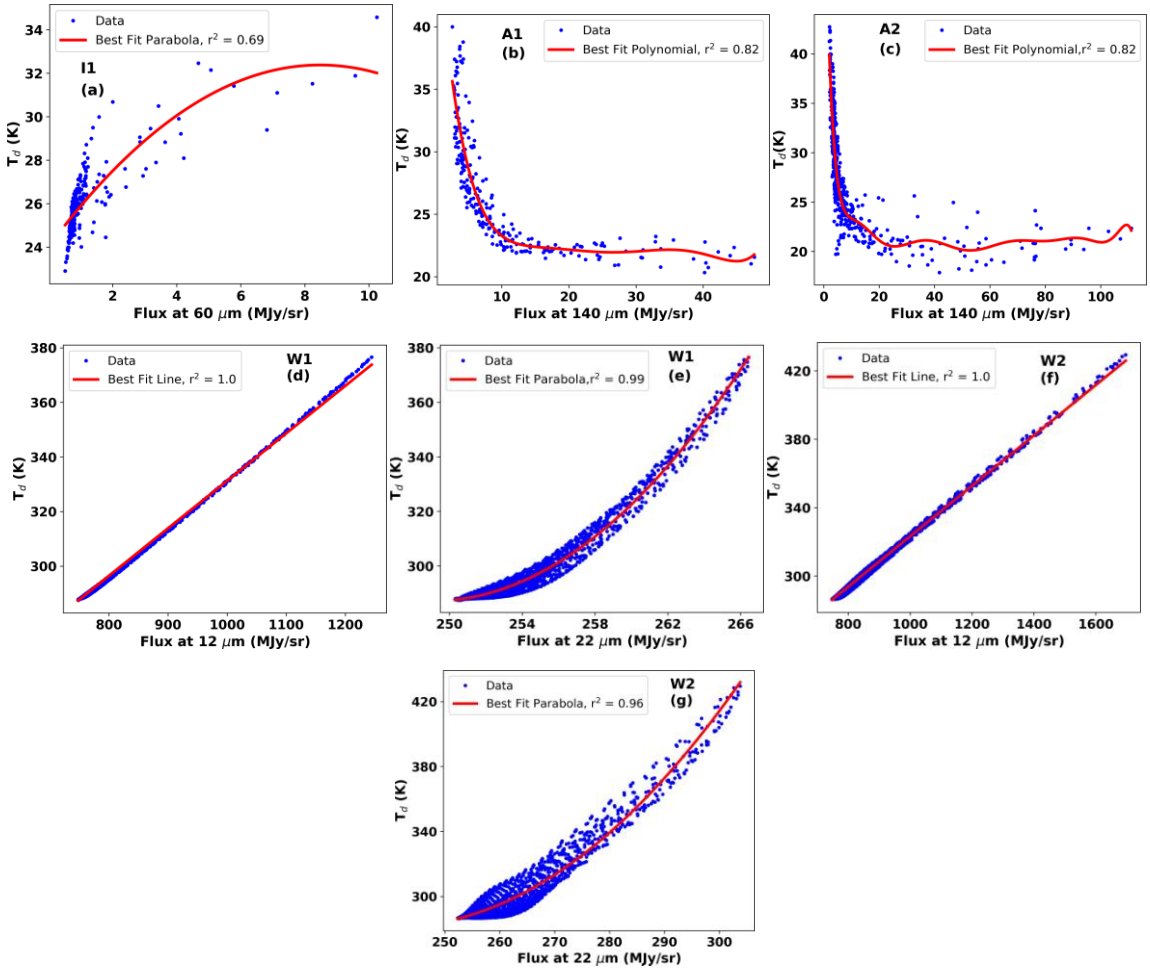

Fig. 6: Figure shows the relation between dust color temperature and infrared flux (60 μm in I1, 140 μm in A1 and A2, 12 μm and 22 μm in W1 and W2).

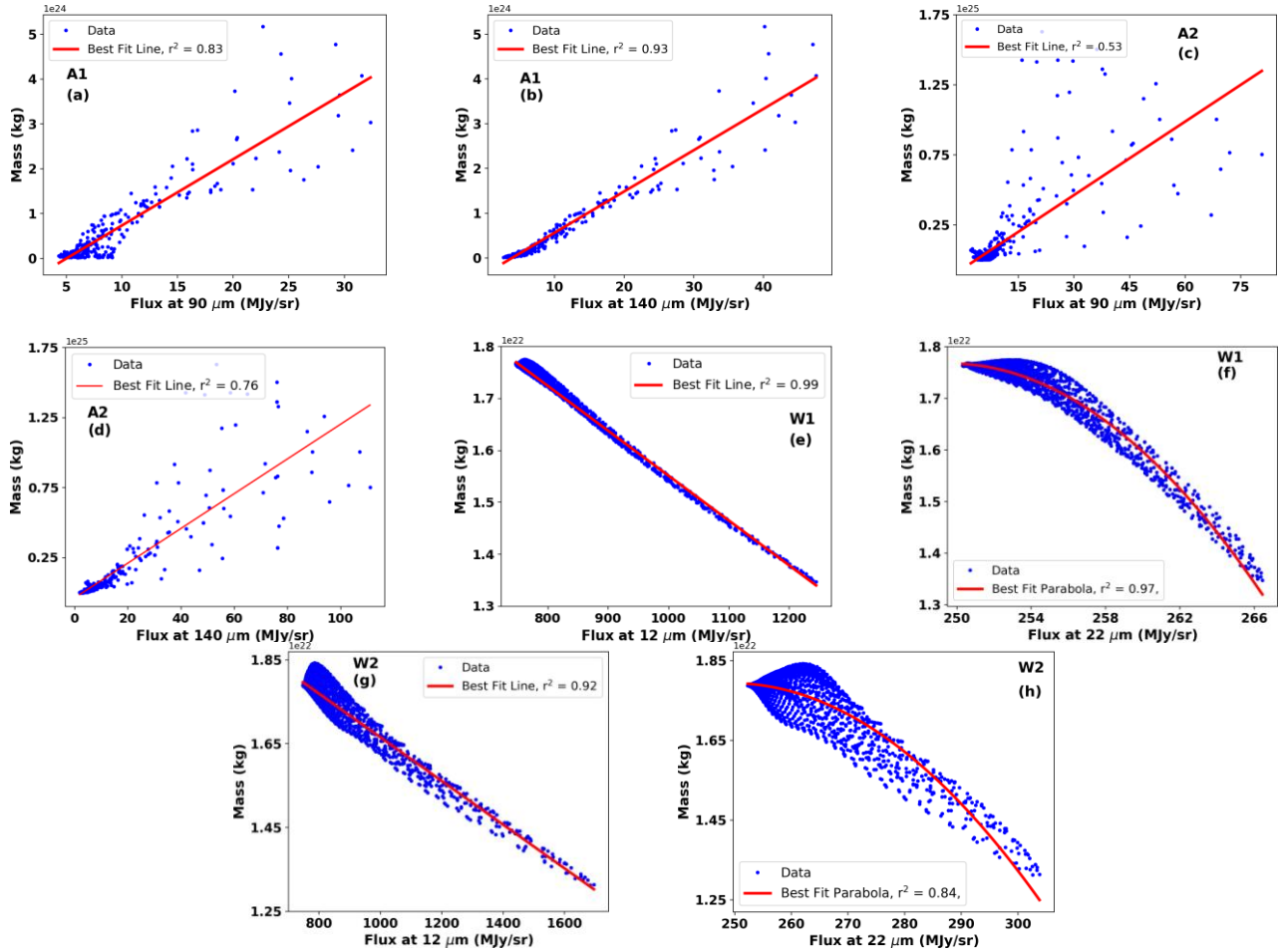

Fig. 7: Figure shows the relation dust mass and infrared flux (90 μm and 140 μm in A1 and A2, 12 μm and 22 μm in W1 and W2).

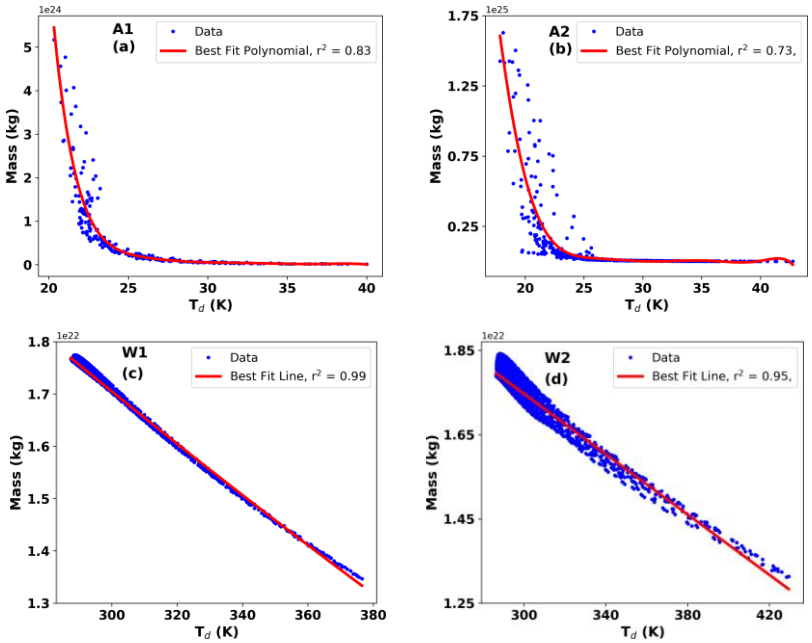

Fig. 8: The figures shows the relationship between the dust color temperature and dust mass in IRIS, AKARI and WISE data in I1, A1, A2, W1 and W2 dust structure.

The White Dwarf PG 1225-079 lies near the center of I1. It is only visible within A2 but not in A1, W1 and W2. Two supernova remnants are seen at the center of bipolar structure; SN 2008ce at the center of A1 and W1, at RA (ICRS): 186.87° and Dec. (ICRS):–8.17° and SN 2010 k at the center of A2 and W2, at RA (ICRS): 186.91° and Dec. (ICRS): −8.28°. These Supernova Remnants might be very important for the source of dust as well as the dust heating energetic radiation within the both sub structures.

Table 6: Object type and their number within rectangular region of size $0.5^0 \times 0.5^0$, the name given in OTYPE are according the symbol in SIMBAD.

OTYPE	Count	OTYPE	Count
Galaxy	20	GinPair	1
Star	5	PairG	1
GroupG	3	EmG	1
PM*	3	WD*	1
IR	2	FIR	1
SN	2		

Gaussian Distribution

The Gaussian distribution with histogram is used to study the normal behavior of the distribution of dust color temperature within the each dust clouds, as given in Fig. 10. The Gaussian distribution is deviated (right skewed) from the normal distribution for I1, very close to normal distribution for A1 and A2 but highly deviated from the normal distribution for W1 and W2. It is evident from the plot of SIMBAD sources around all dust clouds that the number of background sources is very high around I1. This might be the possible reason from the deviation from normal distribution. For the clouds A1, A2, W1 and W2, the number of background sources are very less. The size of the A1 and A2 is larger than the W1 and W2. It can be said that being large in size the effect of the SN 2008ce and SN 2010k is less in A1 and A2 but the effect is more in W1 and W2.

Inclination Angle

The inclination angle is calculated for the isolated region of the infrared flux at a longer wavelength. The major and minor axis of the isolated region within the I1, A1, A2, W1 and W2 are determined from Aladin v2.5 [22] and inclination angle is calculated using Holmberg (1946) formula [20]. The Table 7 presents all the information for the inclination angle. Since, the inclination angle greater than 45^0 represents the *edge-on* and less than $45^{0\circ}$ represents the *face-on* in shape. It is seen that the dust cloud I1 and A2 are *edge-on* in shape, but A1, W1 and W2 are *face-on* in shape.

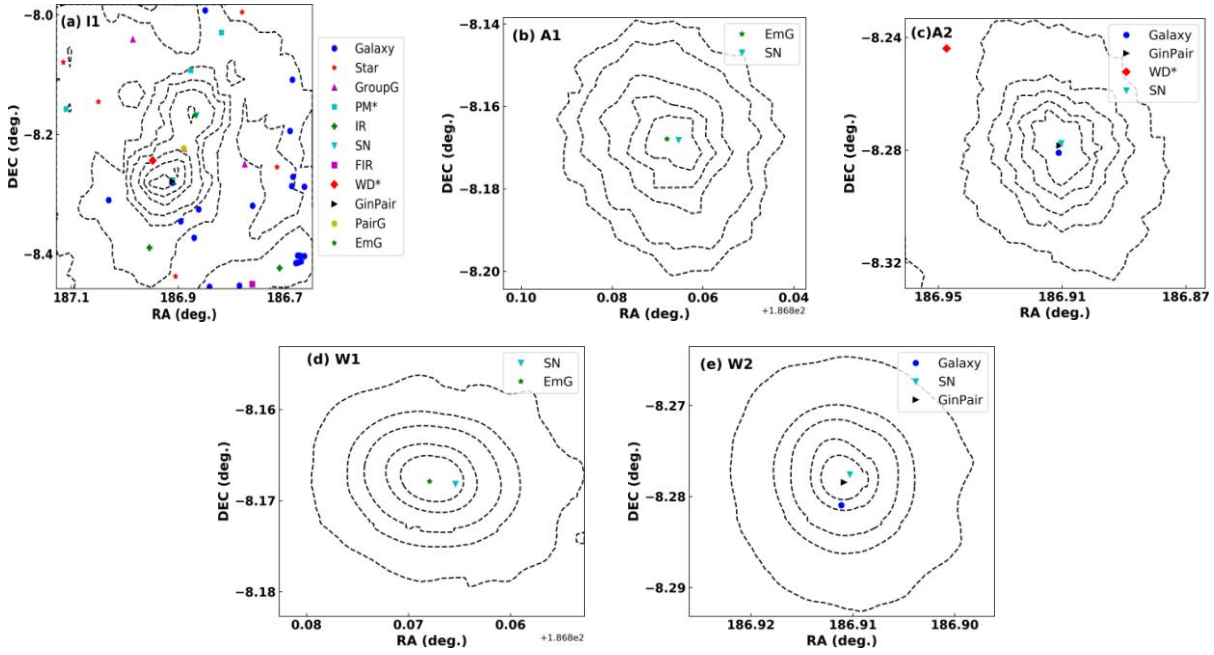

Fig. 9: The SIMBAD objects around the selected dust structure are shown in figure. The contour lines are the isocontours for infrared flux at 100 μm (for I1), 140 μm (for A1, A2) and and 22 μm (for W1, W2).

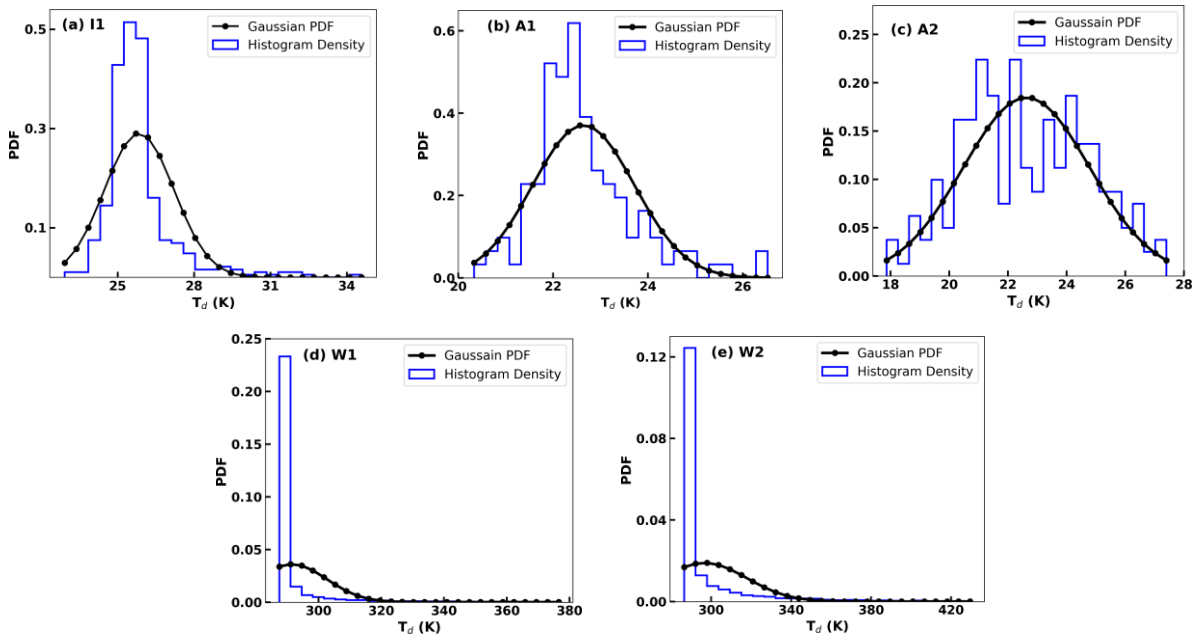

Fig. 10: The figure shows the Gaussian distribution for dust color temperature. In A1 and A2 the distribution is close to normal distribution and for W1 and W2 it is highly deviated from normal shape.

Table 7: The table presents the major axis (*a*), minor axis (*b*), inclination angle (*i*) and shape of the dust cloud I1, A1, A2, W1 and W2.

	a (arcmin)	*b* (arcmin)	*i* (deg)	shape
I1	22.51	10.59	65.09	*edge − on*
A1	3.74	2.74	44.40	*f ace − on*
A2	5.50	3.51	52.31	*edge − on*
W1	1.51	1.28	33.05	*f ace − on*
W2	1.31	1.29	10.31	*f ace − on*

Density and Jeans Mass

The average size, density, average temperature, Jeans mass and total mass of cloud of isolated region within I1, A1, A2, W1 and W2 are presented in Table 8. The size of I1 is obviously larger than all the others, but the density is least. The density is large for W1 and W2. In all dust clouds the Jeans mass M_J is greater than mass of cloud (including gas mass). This suggests that there is no possibility for the collapse of cloud for the process of star formation in the future. The tidal eruption, possibly from Supernova Remnants (SN 2008ce and SN 2010k) is leading the force of gravity to disrupt the cloud further into the process of fragmentation.

Table 8: The table shows the average radius, dust color temperature, density, Jeans mass and total mass of cloud in isolated regions of I1, A1, A2, W1 and W2.

	Radius (m)	T_d (K)	Density (kg/m^3)	Jeans Mass (kg)	Mass of Cloud (kg)
I1	2.43×10^{15}	27.57	2.22×10^{-16}	1.34×10^{31}	1.31×10^{27}
A1	4.76×10^{14}	22.63	4.77×10^{-15}	2.15×10^{30}	3.32×10^{28}
A2	4.76×10^{14}	22.64	1.83×10^{-16}	1.10×10^{31}	1.12×10^{29}
W1	2.05×10^{15}	295.34	3.35×10^{-13}	1.21×10^{31}	1.10×10^{28}
W2	1.91×10^{15}	296.85	3.88×10^{-13}	1.13×10^{31}	1.26×10^{28}

Comparison with Literature

The result obtained in this work fairly matched with the some literature but disagree with some other. The dust color temperature of isolated region in this work is 27.57 K for IRIS data (I1) and 22.64 K and 22.63 K for AKARI data (A1 and A2). The

temperature of the cavity nearby the White Dwarf WD352−249 is 23.09 K in IRAS data [9], which is quite agreement with this work. In a work by Jha and Aryal (2018) [24] the temperature of cavity centered at RA = $05^h05^m35^s$ and Dec. = $-69^0$35' 25" (C1) is found in range 23.4 K to 24.1 K in IRIS and 26.0 K to 28.1 K in AKARI. In the same work, the temperature of cavity centered at RA = $14^h41^m23^s$ and Dec. = $-64^0$04' 17" (C2) is found in range 22.2 K to 24.6 K in IRIS and 25.4 K to 29.7 K in AKARI. The dust color temperature obtained in IRIS data is smaller than in the AKARI data in both cavities C1 and C2 but it is opposite in this work. The distribution of temperature within C_1 and C_2 shows the Gaussian like structure which is similar to this work. The temperature of the dust in nebular structure around the Supernova Remnants G053.41+00.3, G053.9+00.2 and G053.1+00.3 is 25.66 K in IRIS data and 17.74 K in AKARI data [13], which is quite similar to in this work, and the larger value of temperature in IRIS data than in AKARI data is similar to the results obtained in this work. Also, Gaussian distribution of the temperature is deviated slightly from the symmetric nature and it is said that the presence of the high energetic radiation sources including SNR are mainly responsible for the asymmetric distribution [13]. The same trend is followed in this work also; the Gaussian distribution deviated slightly in IRIS (I1) and AKARI (A1 and A2) data but deviated heavily in the WISE data (W1 and W2), which might be due to the presence of the Supernova Remnants at the center of the dust structures. The range of temperature in the cavity structure nearby the White Dwarf WD 1334-678 is 17.70 K to 18.81 K in AKARI data [25], which is quite lower value in comparison to the temperature obtained in this work in AKARI data, possibly due to the nebular structure. Also, the mass of dust per pixels around WD 1334-678 is 1.10×10^{25} kg, which is larger compare to this work.

There is inverse relation between the dust color temperature and dust mass within the dust cavity nearby the White Dwarf WD352-249 [9] and White Dwarf 2236+541 [26]. However, the relation between the dust mass and temperature is mixed type in the dust nebula around the Supernova Remnants G053.41+00.3, G053.9+00.2 and G053.1+00.3[13]. This relation is directly proportional in IRIS data but inversely proportional in AKARI data. But in this work, we have studied the relation between temperature and mass by using the polynomial regression and found that there is no any clear relation in IRIS data and an inverse relation in the AKARI and WISE data.

CONCLUSION

In this work, the infrared flux, dust color temperature and dust mass, Jeans mass and inclination angle of the dust structure around the White Dwarf PG 1225-079 located at RA (J2000): $12^h\ 27^m\ 47.35^s$, DEC(J2000): $-08^0\ 14'\ 37.97"$ [RA (ICRS): 186.87^0, DEC. (ICRS): -08.23^0] is studied. Following are the major conclusions of this research work;

- The average value of dust color temperature in the isolated dust structure I1 is 27.57 K for IRIS data. In AKARI and WISE, the average temperature is 22.64 K for A1, 22.63 K for A2, 295.34 K for W1 and 296.85 K for W2. A wide range of temperatures of more than 5 K in all clouds suggests the bipolar dust clouds are dynamically active.
- The average temperature is found to be increase with decrease in the wavelength following the Wien's displacement law.
- The contour map of infrared flux shows similar types flux distribution across all dust clouds, with high infrared flux at the central part and decreasing outwards.
- The analysis of background sources in the SIM-BAD database reveals several sources, in which the Supernova Remnants; SN 2008ce and SN 2010k are recognized at the center of the bipolar dust structure, which might be the important source of the dust as well as a contributor of energetic radiation responsible for the dust heating.
- The mass of dust in isolated region is found to be 6.53×10^{24} kg in I1, 1.66×10^{26} kg in A1, 5.60×10^{26} kg in A2, 5.48×10^{25} kg in W1 and 6.32×10^{25} kg in W2. The density of the dust is minimum in IRIS and maximum in WISE data.
- The Gaussian distribution of dust color temperature is slightly deviated for I1, very close for A1 and A2 but highly deviated for W1 and W2 compare to the normal distribution. It is concluded that the effect of the SN 2008ce and SN 2010k greater on W1 and W2 compare to A1 and A2.
- The study of inclination angle shows that the dust cloud I1 and A2 are *edge-on* in shape, but A1, W1 and W2 are *face-on* in shape.
- By comparing the Jeans mass with total mass, it

can be concluded that there is no possibility for any star formation activity in future within all dust clouds.

ACKNOWLEDGMENTS

The authors acknowledges the University Grants Commission for funding this research work (award no.: SRDIG 77/78 S&T-5), as well as their host institution, Department of Physics, Tri-Chandra Multiple Campus. Thanks to Sky View Virtual Observatory and SIMBAD database for the data.

REFERENCES

[1] Gehrz, R. D.; Allamandola, L. and Tielens, A. "Interstellar dust," in IAU Symp, *Kluwer Academic Dordrecht*, **135:** 445 (1989).

[2] Barlow, M. J. "The destruction and growth of dust grains in interstellar space–i. destruction by sputtering," *Monthly Notices of the Royal Astronomical Society*, **183:** 367–395 (1978).

[3] Draine, B. T. "Interstellar dust grains," arXiv preprint astro- ph/0304489 (2003).

[4] Karttunen, H.; Kröger, P.; Oja, H.; Poutanen, M. and Donner, K. J. Fundamental astronomy. *Springer*, **4: (**2007).

[5] Neugebauer, G.; Habing, H.; Van Duinen, R.; Aumann, H.; Baud, B. et al. "The infrared astronomical satellite (iras) mission." *The Astrophys- ical Journal*, **278:** L1–L6 (1984).

[6] Murakami, H.; Baba, H.; Barthel, P.; Clements, D. L.; Cohen, M.; et al. "The infrared astronomical mission akari," *Publications of the As- tronomical Society of Japan*, **59**: S369–S376 (2007).

[7] Wright, E. L.; Eisenhardt, P. R.; Mainzer, A. K.; Ressler, M. E.; Cutri, R. M. et al. "The wide-field infrared survey explorer (wise): mission description and initial on-orbit performance." *The Astronomical Journal*, **140:** 1868 (2010).

[8] Thapa, A.; Paudel, M. S. and Pant, B. "An infrared survey of isolated nebular structures at galactic latitudes 16.98° & 1.98° in aras map." *Journal of Nepal Physical Society*, **5:** 74–84 (2019).

[9] Paudel, M. S.; Bhandari, P. and Bhattarai, S. "Study of dust cavity around the white dwarf wd 0352-049 in infrared astronomical satellite map." *Journal of Nepal Physical Society*, **7:** 110–118 (2021).

[10] Paudel, M. S. "Studies of dust properties in substructures around white dwarf wd 0307+077 in iris survey." *Journal of Nepal Physical Society*, **8:** 39–47 (2022).

[11] Jha, A. and Aryal, B. "A study of a cavity nearby a pulsar at-60^{o} latitude in the far infrared map." *Journal of Nepal Physical Society*, **4:** 33–41 (2017).

[12] Jha, A. and Aryal, B. "A study of far infrared loop at-5o galactic lat- itude around pulsar j1627-5547." *BIBECHANA*, **15:** 70–78 (2018).

[13] Paudel, M. S. and Bhattarai, S. "Studies of the properties of dust structure nearby the supernova remnants g053. 41+ 00.3, g053. 9+ 00.2 and g053. 1+ 00.3 using data from iris and akari." *Journal of Nepal Physical Society*, **7**: 59–66 (2021).

[14] Miville-Deschênes, M. A. and Lagache, G. "Iris: a new generation of iras maps." *The Astrophysical Journal Supplement Series*, **157:** 302 (2005).

[15] Wood, D. O.; Myers, P. C. and Daugherty, D. A. "Iras images of nearby dark clouds." *The Astrophysical Journal Supplement Series*, **95:** 457–501 (1994).

[16] Schnee, S. L.; Ridge, N. A.; Goodman, A. A. and Li, J. G. "A complete look at the use of iras emission maps to estimate extinction and dust temperature." *The Astrophysical Journal*, **634**: 442 (2005).

[17] Dupac, X.; Bernard, J. P.; Boudet, N.; Giard, M.; Lamarre, J. M. et al., "Inverse temperature dependence of the dust submillimeter spectral index." *Astronomy & Astrophysics*, **404**: L11–L15 (2003).

[18] Young, K.; Phillips, T. and Knapp, G. "Circumstellar shells resolved in iras survey data. ii-analysis." *The Astrophysical Journal*, **409:** 725–738 (1993).

[19] Hildebrand, R. H. "The determination of cloud masses and dust characteristics from submillimetre thermal emission." *Quarterly Journal of the Royal Astronomical Society*, **24**: 267 (1983).

[20] Holmberg, E. "On the apparent diameters and the orientation in space of extragalactic nebulae." Meddelanden fran Lunds Astronomiska Observatorium Serie II, **117:** 3–82 (1946).

[21] Haynes, M. P. and Giovanelli, R. "Neutral hydrogen in isolated galaxies. iv-results for the arecibo sample." *The Astronomical Journal*, **89**: 758–800 (1984).

[22] Bonnarel, F.; Fernique, P.; Bienaymé, O.; Egret, D.; Genova, F. et al. "The al- adin interactive sky atlas-a reference tool for identification of astro-nomical sources." *Astronomy and Astrophysics Supplement Series*, **143**: 33–40 (2000).

[23] Collaboration, G. "Vizier online data catalog: Gaia edr3 (gaia col- laboration, 2020)," VizieR Online Data Catalog, I/350 (2020).

[24] Jha, A. and Aryal, B. "Dust color temperature distribution of two fir cavities at iris and akari maps." *Journal of Astrophysics and Astronomy*, **39**: 1–7 (2018).

[25] Joshi, I. N.; Jha, A. K. and Aryal, B. "A study of dust structure nearby white dwarf wd1334-678." *BIBECHANA*, **18**: 130–137 (2021).

[26] Sapkota, B. and Aryal, B. "A study of far infrared cavity at-3.6 galactic latitude." *Journal of Nepal Physical Society*, **5**: 54–58 (2019).

[27] Assendorp, R. and Wesselius, P. "Iras pointed observations data processing," Astronomy and Astrophysics Supplement Series, **100**: 473–488 (1993).